Nonlinear all-optical switch based on a white-light cavity

Na Li,[1] Jingping Xu,[1,2,*] Ge Song,[1,4] Chengjie Zhu,[1] Shuangyuan Xie,[1] Yaping Yang,[1,†]
M. Suhail Zubairy,[2,3] and Shi-Yao Zhu[2]

[1]*MOE Key Laboratory of Advanced Micro-Structured Materials, School of Physics Science and Engineering, Tongji University, Shanghai 200092, People's Republic of China*

[2]*Beijing Computational Science Research Center, Beijing 100084, People's Republic of China*

[3]*Institute of Quantum Science and Engineering (IQSE) and Department of Physics and Astronomy, Texas A&M University, College Station, Texas 77843-4242, USA*

[4]*School of Aerospace Engineering and Applied Mechanics, Tongji University, Shanghai 200092, People's Republic of China*

(Received 25 January 2016; published 12 April 2016)

It is well known that there is a bottleneck for nonlinear all-optical switching, namely, the switching power and the switching time cannot be lowered simultaneously. A lower switching power requires a resonator with a high quality (Q) factor, but leads to a longer switching time. We propose to overcome this bottleneck by replacing the nonlinear cavity in such an all-optical switch by a white-light cavity. This can be done by doping three-level atoms in the ring resonator and applying incoherent pump and coherent driving fields on it. The white-light cavity possesses broadband resonance in a linear region. Therefore, for the incident pulse, a broad range of frequency components can take part in the nonlinear process, and so it requires lower power to achieve switching compared to the conventional ring resonator. On the other hand, the refractive index of a white-light cavity has negative dispersion, leading to a fast group velocity. This results in a shorter time to build up the resonant response, yielding a short switching time.

DOI: 10.1103/PhysRevA.93.043819

I. INTRODUCTION

In recent decades, the development of optical technology [1] in the field of information transfer and storage has led to a replacement of many electronic devices by optical devices [2,3]. However in the field of information processing the electronics technology still dominates. This is due to the difficulties in replacing the electronic switch (or transistor) by a photonic switch (or a phototransistor). In principle, all-optical switches based on the optical nonlinearity of materials possess unique advantages, such as lower loss and a fast response, superior to those of electric switches [4]. Therefore it is anticipated that an all-optical switch will be a key element for future optical communications and optical computation [4].

Nonlinear optical switches are based on the nonlinear optical properties of media which can change the output state of the signal light through a controllable pump or the signal light itself. This type of switch requires strong field intensity to generate third-order nonlinearity. However, a switch driven by a strong field cannot be used in a cascade system as the system can become very unstable. To realize a lower-power optical switch, a high-Q resonator can be used to amplify the field in the resonator under weak field input.

Here we consider a fiber ring resonator because of its simple structure and compatibility with the present fiber network. Urquhart proposed the fiber ring cavity structure [5], which has the advantage of enhancing nonlinearity, but the losses are also increased. Subsequently the ring resonator [6] has been widely applied in all kinds of optical switching structures [7,8]. In order to compensate the losses, Bananej and Li suggested using an erbium-doped fiber (EDF) to make part of the ring to compensate the loss through the pump, and finally formed an annular optical amplifier [9]. On this basis, Li proposed an active double-coupled ring resonator (DCRR) [10] all-optical switch, in which half of the fiber ring is made by a 980-nm-laser-pumped erbium-doped fiber to form an erbium-doped fiber amplifier (EDFA) [11]. This structure can further reduce the device size, allowing high-density integration.

In this paper we adopt the ring resonator as an example to give our suggestion which can break the bottleneck presented in all resonator-based nonlinear optical switches. The bottleneck is that switching power and switching time cannot be reduced simultaneously. In practice all-optical switches must be low power, high speed, and low loss. Low threshold switching power requires a high-Q cavity [12]. However the time required to build up the resonant response (or decay of the resonant response) in the ring resonator also depends on its quality factor [13]. That means that, when the Q value of the cavity is high, the time required to establish a steady state is very long, leading to a low switching speed. Therefore we want to provide a way to deal with this dilemma with the help of a white-light cavity.

Unlike the conventional cavity possessing discrete resonant frequencies, when the cavity is filled with a negative-dispersion medium, it is possible to realize a continuous range of the spectrum resonating at the same time. Such a special cavity with broadband resonance is called a white-light cavity [14]. Initially white-light cavities were suggested in order to achieve precision measurements such as gravitational wave detection [15,16] and ring laser gyroscopes [17]. Usually high sensitivity requires both high finesse and wide bandwidth of the cavity, but high finesse leads to a narrow bandwidth in a conventional cavity. So only a white-light cavity can provide an effective way to increase the bandwidth and solve this dilemma. Three-level Λ atomic systems with appropriate driving fields applied can be used to get negative dispersion

*xx_jj_pp@hotmail.com
†yang_yaping@tongji.edu.cn

with a gain doublet and construct white-light cavity [18–22]. Among them, we proposed to realize a white-light cavity through a Fabry-Pérot cavity filled with a gas of three-level atoms applied by incoherent pump and coherent driving fields [22].

In this paper, we combine a white-light ring cavity with a nonlinear double-coupled ring resonator. This will allow the switching power to be reduced and the switching speed to be improved at the same time. When the two most important performance parameters are not contradictory, low-power ultrafast nonlinear all-optical switch in a double-coupled ring resonator can be achieved.

The paper is organized as follows: In Sec. II, we introduce the parameters and properties of the present double-coupled nonlinear ring resonator all-optical switch. In Sec. III, we improve the ring resonator by doping it with three-level atoms to achieve a white-light cavity with appropriate pump and driving fields. In Sec. IV, we analyze the performance of the nonlinear optical switch based on a white-light cavity, i.e., the switching power and switching speed. The conclusion is presented in Sec. V.

II. DOUBLE-COUPLED NONLINEAR RING RESONATOR ALL-OPTICAL SWITCH

The configuration of the all-optical switch based on a nonlinear ring cavity [11] is shown in Fig. 1. A ring fiber is coupled with two straight waveguides through the couplers C_1 and C_2. We denote the reflection and transmission coefficients of coupler $C_i (i = 1,2)$ by r_i and t_i, respectively. They satisfy the relationship $r_i^2 + t_i^2 = 1$. Half of the ring is made of silica fiber of length l_2, and the rest is erbium-doped fiber of length l_1. The total length of the ring resonator is $l = l_1 + l_2$. The dissipation of the switch includes the insertion losses of coupler C_i, γ_i, losses in the EDF and silica fiber, η_i, and their absorption coefficients per unit length α_i $(i = 1,2)$. To compensate these losses, the EDF is pumped by 980 nm light through wavelength division multiplexing (WDM) with gain G. The linear index of the fiber (both the EDF and silica fiber) is $n_1 = 1.5$, and the nonlinear refractive coefficients are n_{21} ($\approx 10^{-15}$ m^2/W) for the EDF and n_{22} ($\approx 10^{-20}$ m^2/W) for silica.

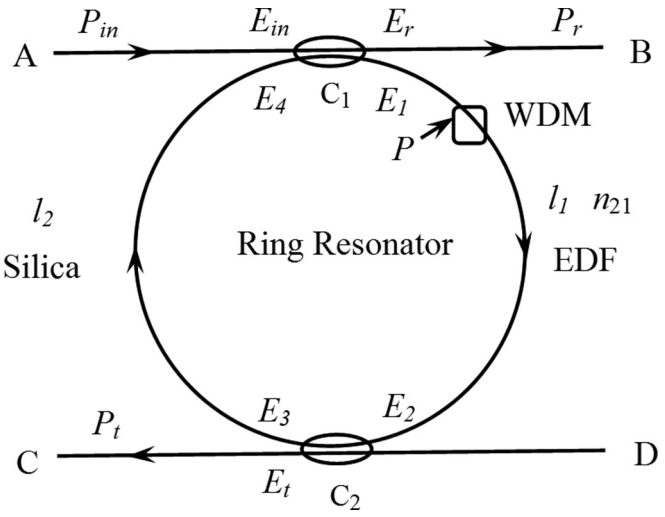

FIG. 1. Scheme of a nonlinear all-optical switch in a double-coupled nonlinear ring resonator.

Typical values of the dissipation parameters are $\gamma_1 = \gamma_2 = 0.05$, $\eta_1 = 0.2$, $\eta_2 = 0.005$, $\alpha_1 = 0.7$ m^{-1}, and $\alpha_2 = 7 \times 10^{-5}$ m^{-1} [11] and the length of the ring is $l = 3.1 \times 10^{-5}$ m. To compensate the dissipation, we tune the gain to the value $G = 1.392$, so that

$$\sqrt{G(1-\eta_1)(1-\eta_2)(1-\gamma_1)(1-\gamma_2)e^{-(\alpha_1 l_1+\alpha_2 l_2)}} \approx 1, \quad (1)$$

and the losses in the switch can be ignored.

When a continue wave (cw) signal with power $P_{\rm in} = |E_{\rm in}|^2$ and frequency ω_0 is launched into port A, the signal passes through the couplers C_1 and C_2 successively, and is finally output at port C with power $P_t = |E_t|^2$ and port B with power $P_r = |E_r|^2$. Under the condition of Eq. (1) and ignoring all losses, the reflection R, transmission T, and intracavity amplification M of the switch can be simplified as

$$R(\omega) = \left|\frac{E_r}{E_{\rm in}}\right|^2 = \frac{r_1^2 - 2r_1 r_2 \cos(\varphi) + r_2^2}{1 - 2r_1 r_2 \cos(\varphi) + r_1^2 r_2^2}, \quad (2)$$

$$T(\omega) = \left|\frac{E_t}{E_{\rm in}}\right|^2 = 1 - R(\omega), \quad (3)$$

$$M(\omega) = \left|\frac{E_2}{E_{\rm in}}\right|^2 = \frac{T(\omega)}{t_2^2}. \quad (4)$$

Here φ is the single-pass phase shift in the ring, and is a purely real value for this lossless case. It can be divided into two parts: the linear part φ_0 and the nonlinear part $\Delta\varphi$, i.e., $\varphi = \varphi_0 + \Delta\varphi$. The linear part is given by

$$\varphi_0 = \frac{\omega_0}{c} n_1 l. \quad (5)$$

As the nonlinear refractive index of the EDF ($n_{21} \approx 10^{-15}$ m^2/W), is much larger than that of the silica fiber ($n_{22} \approx 10^{-20}$ m^2/W), the nonlinear part can be expressed as

$$\Delta\varphi = \frac{\omega_0 n_{21} l_1}{c}\frac{P_2}{S} + \frac{\omega_0 n_{22} l_2}{c}\frac{P_4}{S} \approx \frac{\omega_0 n_{21} l_1}{c}\frac{P_2}{S} = \frac{\omega_0 n_{21} l M P_{\rm in}}{2cS}, \quad (6)$$

where $P_{2(4)} = |E_{2(4)}|^2$ is the circulating clockwise power for coupler C_2 (C_1). Please note P_2 is the power without nonlinearity. In the last step in Eq. (6), $P_2(\Delta\varphi = 0) = M(\Delta\varphi = 0)P_{\rm in}$, according to Eq. (4), is used. Here S is the effective cross section of the ring cavity. From now on, we set $n_{21} = 3.5 \times 10^{-15}$ m^2/W and $S = 1.5 \times 10^{-13}$ m^2.

The wavelength of the signal is $\lambda_0 = 1550$ nm ($\omega_0 = 2\pi c/\lambda_0$). As $l = 20\lambda_0$ and $n_1 = 1.5$, the linear phase shift φ_0 is an integral multiple of 2π and the resonance condition is satisfied. We consider the case of $r_1 = r_2 = r_c$ and $r_c \to 1$.

When the input power is relatively small, the nonlinear effects can be ignored and, with $\varphi = \varphi_0 = 60\pi$, we obtain

$$M(\Delta\varphi = 0) = \frac{1}{1 - r_c^2}, \quad R(\Delta\varphi = 0) = 0, \quad T(\Delta\varphi = 0) = 1. \quad (7)$$

The signal is extracted at port C with $P_r = 0$ and $P_t = P_{\text{in}}$. This corresponds to the "off" state of the switch.

If the input power increases, the nonlinear effects become important. We consider the case when the induced Kerr effect is such that the resulting nonlinear phase shift is $\Delta\varphi = \pi$. We then obtain

$$R(\Delta\varphi = \pi) \approx 1, \quad T(\Delta\varphi = \pi) \approx 0, \tag{8}$$

i.e., the signal is extracted at port B with $P_r = P_{\text{in}}$ and $P_t = 0$. This refers to the "on" state of the switch. Therefore, the switching condition for such a nonlinear switch is $\Delta\varphi = \pi$.

In order to achieve $\Delta\varphi = \pi$ for single-frequency incident light, the switching power should be [11]

$$P_{\text{inc}} = \frac{\lambda S}{n_{21} l M(\Delta\varphi = 0)} = \frac{\lambda S}{n_{21} l Q T(\Delta\varphi = 0)} = \frac{\lambda S}{n_{21} l Q}, \tag{9}$$

where Q is the quality factor of the cavity [23], which satisfies

$$Q = \frac{|E_2|^2}{|E_t|^2} = \frac{M}{T}. \tag{10}$$

We note that, on resonance, M is equal to Q, i.e., $Q = M$ $(\Delta\varphi = 0)$, because in this case $|E_t|^2 = |E_{\text{in}}|^2$ and $T = 1$.

Another important performance parameter of the optical switch is the switching time. The switching time τ depends on both the material response time τ_f and the ring cavity lifetime τ_c, i.e., $\tau = \tau_c + \tau_f$. The response time of an EDF at $\lambda_0 = 1550$ nm is of the order of subnanoseconds [24]. In contrast, the cavity lifetime τ_c is the time needed for the field accumulation in the cavity, which is proportional to the quality factor Q as [11]

$$\tau_c = \frac{n_1 l Q}{c} = \frac{n_1 l}{\lambda_0} Q \tau_0. \quad \text{with} \quad \tau_0 = \frac{\lambda_0}{c}. \tag{11}$$

Usually $\tau_c \gg \tau_f$, and therefore the switching time is determinated by the cavity lifetime τ_c only. In the above equation τ_0 is *the period of the input field* and is chosen as the unit of time in this paper.

On comparing Eqs. (9) and (11), it is clear that decreasing the switching power through a high-Q cavity results in prolonging the switching time. It is difficult to reduce the switching power and, at the same time, decrease the switching time. This reciprocity between the switching power and the switching time is a bottleneck of nonlinear all-optical switches.

We show in the next sections how it is possible to use a white-light cavity to overcome this problem. However, before discussing the role of white-light cavities, we present how a driven three-level atomic system can lead to a white-light cavity with a broadband resonance.

III. WHITE-LIGHT CAVITY

For a conventional cavity, there are discrete frequencies which satisfy the resonance condition

$$\text{Re}(n_1)\frac{\omega_{\text{res}}}{c} l = 2m\pi, \quad (m = 1,2,\ldots). \tag{12}$$

In order to realize broadband resonance, we need negative dispersion for the index of refraction n_1. In addition, the imaginary part of n_1 should also be eliminated to avoid detuning.

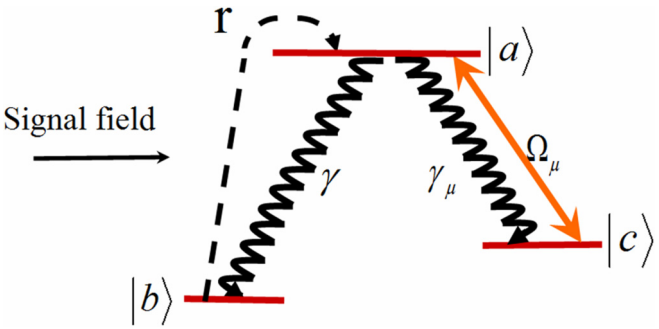

FIG. 2. Level scheme of the doped three-level atom.

We follow our previous work [22] to realize the white-light ring cavity. Three-level atoms with the configuration shown in Fig. 2 are homogeneously doped inside the ring resonator.

The transition frequency ω_{ab} associated with the $|a\rangle \leftrightarrow |b\rangle$ transition is chosen to be resonant with the ring resonator, i.e., $\omega_{ab} = \omega_0$. The transition $|a\rangle \leftrightarrow |b\rangle$ interacts with the signal field, and provides an alternative linear susceptibility χ. This susceptibility is controllable through external fields. For example, the coherent driving field with Rabi frequency Ω_μ is coupled with the transition $|a\rangle \leftrightarrow |c\rangle$ resonantly. In addition, an incoherent field is used to pump the atoms from level $|b\rangle$ to level $|a\rangle$ with a pumping rate r. The decay rates from level $|a\rangle$ to $|b\rangle$ and from level $|a\rangle$ to $|c\rangle$ are denoted by γ and γ_μ, respectively. The decay rate from level $|c\rangle$ to $|b\rangle$ is ignored.

According to Refs. [22,25], the susceptibility of the doping atoms can be expressed as

$$\chi(\omega) = A\frac{[(\omega_{ab} - \omega) - i\gamma_{cb}]\left(\rho_{aa}^{(0)} - \rho_{bb}^{(0)}\right) + \Omega_\mu \rho_{ca}^{(0)}}{[|\Omega_\mu|^2 - (\omega_{ab} - \omega)^2 + \gamma_{ab}\gamma_{cb}] + i(\omega_{ab} - \omega)(\gamma_{cb} + \gamma_{ab})}, \tag{13}$$

where $A = N d_{ab}^2/\varepsilon_0\hbar$ with N being the number density of doping atoms and d_{ab} being the dipole moment of the transition $|a\rangle \leftrightarrow |b\rangle$. For a weak signal field, the steady-state values of $\rho_{aa}^{(0)}$, $\rho_{bb}^{(0)}$, and $\rho_{ca}^{(0)}$ are obtained as follows:

$$\rho_{aa}^{(0)} = \frac{2r|\Omega_\mu|^2}{2(2r + \gamma)|\Omega_\mu|^2 + r\gamma_\mu\gamma_{ca}}, \quad \rho_{bb}^{(0)} = \frac{\gamma}{r}\rho_{aa}^{(0)},$$
$$\rho_{ca}^{(0)} = \frac{-i\Omega_\mu^*\left(1 - 2\rho_{aa}^{(0)} - \rho_{bb}^{(0)}\right)}{\gamma_{ca}}. \tag{14}$$

The decay rates in Eq. (14) are defined as $\gamma_\mu = 0.2\gamma$, $\gamma_{ca} = (\gamma + \gamma_\mu)/2$, $\gamma_{ab} = (r + \gamma + \gamma_\mu)/2$, and $\gamma_{cb} = r/2$. For lower density of the doping atoms, we set $A = \gamma$ in Eq. (13).

When the pump is applied and its pumping rate is larger than the decay rate, i.e., $r > \gamma$, the susceptibility will show negative dispersion near ω_{ab} $(=\omega_0)$. Furthermore the imaginary part of the susceptibility is approximately equal to zero in the presence of the coherent driving field Ω_μ. In Fig. 3, we plot the susceptibility of such a three-level atom system with the pumping rate $r = 2\gamma$ and the driving field $\Omega_\mu = 8\gamma$.

In order to realize a white-light cavity, the parameters must be optimized to satisfy the equation [15,22]

$$\partial \text{Re}[n(\omega)]/\partial\omega|_{\omega=\omega_{ab}} = -n(\omega_{ab})/\omega_{ab}. \tag{15}$$

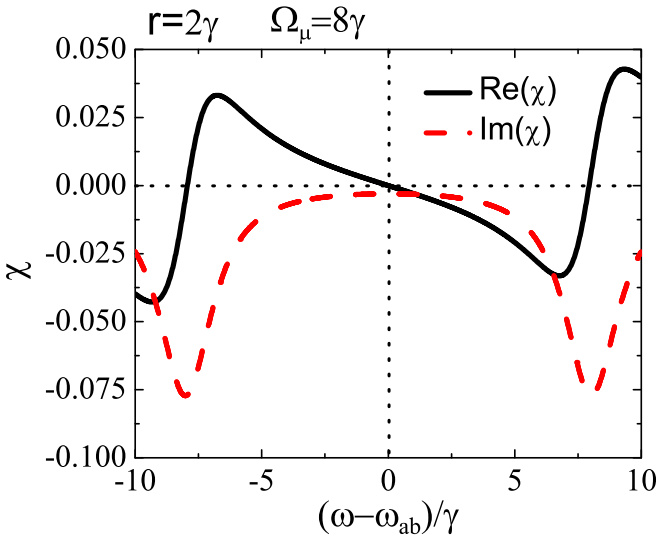

FIG. 3. Susceptibility as a function of the frequency of the signal field for pumping rate $r = 2\gamma$ with $\Omega_\mu = 8\gamma$. $\gamma = 2\pi \times 4.6$ MHz [26].

The linear index of the doped ring can be expressed as

$$n(\omega) = \sqrt{2.25 + \chi(\omega)}. \tag{16}$$

Here 2.25 originates from the index of the ring fiber $n_1 = 1.5$. Following the same procedure as adopted in Ref. [22], we can obtain a condition involving the pumping rate r and the driving field $\Omega_{\mu W}$ to realize broadband resonance.

To confirm the prediction, we calculate the reflection R and intracavity amplification M as functions of frequency in Fig. 4 for the ring cavity doped with a three-level atom system with $\varphi(\omega) = n(\omega)l\omega/c$ in the linear region with $n(\omega)$ defined in Eq. (16). As the index $n(\omega)$ is complex here, the amplification M should be redefined as

$$M(\omega) = \left| \frac{t_1 e^{i\varphi(\omega)/2}}{1 - r_1 r_2 e^{i\varphi(\omega)}} \right|^2. \tag{17}$$

From Fig. 4(a), it is clear that, when the pump and driving field satisfy the white-light cavity condition, i.e., $r = 4\gamma$ and $\Omega_{\mu W} = 333.31\gamma$, there is a wide band with a width of about 300γ in which the reflection is near 0, which means broadband resonance. As a comparison, the reflection of a conventional ring cavity without doping shows a valley shape at the exact resonance $\omega_{ab} = \omega_0$. The FWHM of the white-light cavity is about 400γ while that of a conventional ring resonator is 120γ.

In Fig. 4(b), we plot the spectrum of the intracavity amplification M. This also shows broadband resonance for the white-light cavity. In addition, $M(\omega_{ab})$ in the white-light cavity is about 102, while $M(\omega_{ab})$ in a conventional cavity is 100. They are nearly the same which means that their Q factors are nearly the same. The reason why $M(\omega_{ab})$ in the white-light cavity is a little larger than that in a conventional cavity is that there is a tiny negative imaginary part of χ near ω_{ab} in the white-light cavity as shown in Fig. 3. As the white-light cavity has a broadband resonance, if the wave packet is used as the signal field, its broadband components can all be resonant inside the ring and take part in the nonlinear process.

IV. NONLINEAR SWITCH BASED ON WHITE-LIGHT CAVITY

In this section, we analyze the performance of the nonlinear double-coupled ring resonator switch based on a white-light cavity. To show its advantages, we compare the performance of this type of switch with the conventional optical switch. In realistic cases, the signal field is not exactly cw, but a very long pulse. Therefore we adopt the pulse as the incident signal field to check the two complementary characteristics of the switch, namely, the switching power and the switching time.

A. Switching power

We consider the incident signal field to be a Gaussian pulse with center frequency ω_0, whose spectral distribution is

$$\rho(\omega) = \frac{\tau}{2\sqrt{\pi}} e^{-\tau^2(\omega-\omega_0)^2/4}, \tag{18}$$

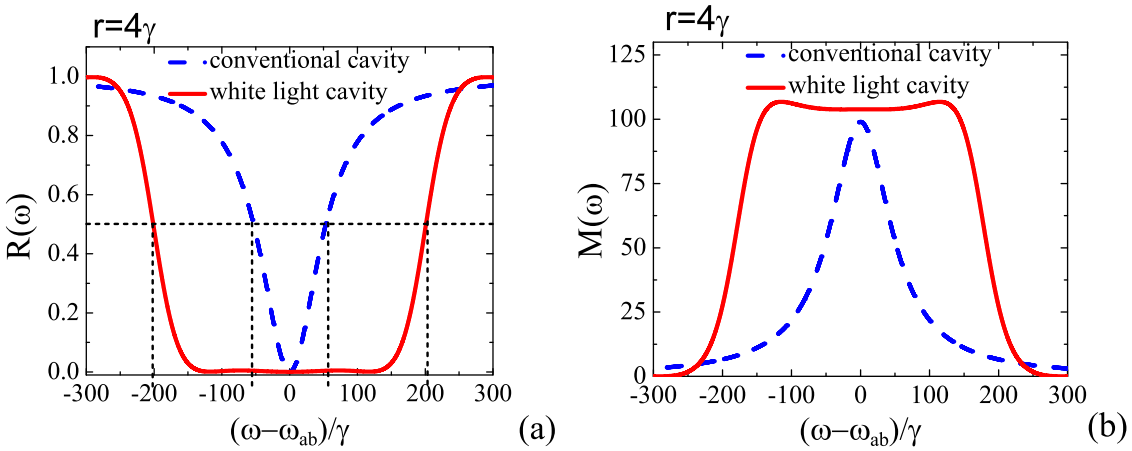

FIG. 4. (a) Reflection R and (b) intracavity amplification M of the ring cavity as a function of the frequency of the signal field. The red solid curves correspond to the white-light cavity with $r = 4\gamma$ and $\Omega_{\mu W} = 333.31\gamma$. The blue dashed curves refer to the conventional ring cavity without doping with a three-level atom. $r_c^2 = 0.99$. $\gamma \approx 2\pi \times 4.6$ MHz.

where τ is the duration of the pulse that determines the spectral distribution. The incident wave packet at the incident position can be expressed as follows [27]:

$$E_i(t) = E_0 \int_0^{+\infty} \rho(\omega) e^{-i\omega t} d\omega. \tag{19}$$

The power of the incident wave packet can therefore be written as

$$P_i(t) = P_0 \left(\frac{\tau}{2\sqrt{\pi}}\right)^2 \left| \int_0^{\infty} e^{-\tau^2(\omega-\omega_0)^2/4 - i\omega t} d\omega \right|^2, \tag{20}$$

where $P_0 \propto |E_0|^2$ represents the peak power of the pulse.

When the pulse is launched at port A, it can be partially coupled into the ring cavity, and finally exits after propagating through the ring. The phase shift per circle for each frequency component can be expressed as

$$\varphi(\omega) = \varphi_0 + \Delta\varphi = \frac{\omega}{c} n(\omega) l + \frac{\omega n_{21} l P_2}{2cS}, \tag{21}$$

where

$$P_2 = P_0 \left| \int_0^{\infty} \sqrt{M(\omega)} \rho(\omega) d\omega \right|^2. \tag{22}$$

is the peak power of the pulse inside the ring cavity. Here M is defined in Eq. (17). The first part of Eq. (21), i.e., $n(\omega)l\omega/c$, is almost a constant in a white-light cavity. Nonlinearity is embodied in the second part. The frequency components that are resonant with the cavity can be amplified inside the cavity and take part in the nonlinear Kerr effect, which leads to a phase shift and results in an "on" switch. On the other hand, those frequency components that are detuned with respect to the cavity cannot be coupled into the cavity and have no contribution to the switch. To achieve a certain P_2 which can leads to a π phase shift, the required input power P_0 [defined in Eq. (20)] for the white-light cavity is smaller than that for a conventional cavity according to the result of Fig. 4(b). This is the reason why a white-light cavity can realize a lower switching power than the conventional optical switch.

To confirm our prediction, we define the reflection of the pulse at port B as

$$R = \frac{I_0 \left| \int_0^{\infty} R(\omega)\rho(\omega) d\omega \right|^2}{I_0 \left| \int_0^{\infty} \rho(\omega) d\omega \right|^2}. \tag{23}$$

Here $R(\omega)$ is given in Eq. (2). With Eqs. (18) and (21)–(23), we plot the total reflection R as a function of incident peak power P_0 in Fig. 5.

In Figs. 5(a), 5(c), and 5(e), we plot the total reflection R as a function of the incident peak power of the pulse P_0 for three incident pulses with $\tau = 800\tau_0$, $\tau = 1200\tau_0$, and $\tau = 3000\tau_0$. For comparison, we denote the result for the white-light cavity with the red solid curve, while that of the conventional ring resonator is given as a blue dashed curve.

It is clear that, when the input power is weak, i.e., $P_0 = 0$, the reflection of a switch based on a white-light cavity is lower and it is in the "off" state. Meanwhile the reflection of a conventional-resonator-based switch is not lower; it increases with shorter τ, i.e., $R = 0.2$ for $\tau = 3000\tau_0$, $R = 0.5$ for $\tau = 1200\tau_0$, and $R = 0.63$ for $\tau = 800\tau_0$. The reason is that the FWHM of the conventional resonator is smaller than that of the incident pulse. Thus a shorter value of τ leads to a larger FWHM of the pulse. In Figs. 5(b), 5(d), and 5(f), we denote the spectrum of the pulse as a black solid curve, the transmission spectrum of the conventional resonator as a blue dashed curve, and that of the white-light cavity as a red dash-dotted curve. For the incident pulse, frequency components detuned from the resonator cannot enter into the ring and should be reflected to port B directly. Therefore the reflection at port B is not equal to zero for conventional resonators. This phenomenon also happens for white-light cavities, but it is not apparent because of the broadband resonance in the cavity. In practice, we can add a filter at port B to filter out the nonresonance spectrum.

The reflection increases monotonically with increase of the incident power. When the input power increases to a certain value, the reflection is close to 1, which switches the resonator to the status "on". We define the incident power which makes the reflection reach 0.99 as the switching power, i.e., P_{inc}. Because the spectral components of the pulse that are resonant with the white-light cavity are much larger than those for a conventional resonator, the switching power for the switch based on the white-light cavity is always smaller than that for the conventional switch. This is evident by comparing the solid curves with the dashed curves in Figs. 5(a), 5(c), and 5(e). For example, under the incident pulse with $\tau = 800\tau_0$, $\tau = 1200\tau_0$, and $\tau = 3000\tau_0$, the switching powers of the all-optical switch based on the white-light cavity are only $P_{\text{inc}} = 10$ mW, $P_{\text{inc}} = 4$ mW, and $P_{\text{inc}} = 0.8$ mW. By contrast, the switching powers for the conventional switch are $P_{\text{inc}} = 30$ mW, $P_{\text{inc}} = 12$ mW, and $P_{\text{inc}} = 2.5$ mW.

The switching power for the white-light-cavity-based switch also changes with incident pulses with different durations τ because the bandwidth of the white-light cavity is limited to 400γ. In conclusion the white-light cavity is helpful in reducing the switching power compared to the conventional resonator. In our simulation here, this reduction is nearly by a factor of 1/3.

B. Switching time

Next we study the switching time. It should be noticed that Eq. (11), i.e., $\tau = nlQ/c$, is valid only for cw incidence. It refers to the time for single-frequency cavity field building. When Q is high, the cavity field will run many circles inside the ring before it escapes out of the cavity, so the time for cavity field building is prolonged. At such times, the cavity field reaches its peak value and leads to apparent nonlinear effects, and then the switch works. Therefore the time for cavity field building is just the switching time.

The switching time changes when the input signal is a pulse. Here we adopt the pulse evolution to check the switching time, and compare the case of the white-light cavity with that of the conventional resonator. The calculations are focused only on the linear regime.

The incident pulse is expressed in Eq. (20). The transmitted pulse at port C is

$$I_t(t) = \left(\frac{\tau}{2\sqrt{\pi}}\right)^2 \left| \int_0^{\infty} t(\omega) e^{-\tau^2(\omega-\omega_0)^2/4 - i\omega t} d\omega \right|^2, \tag{24}$$

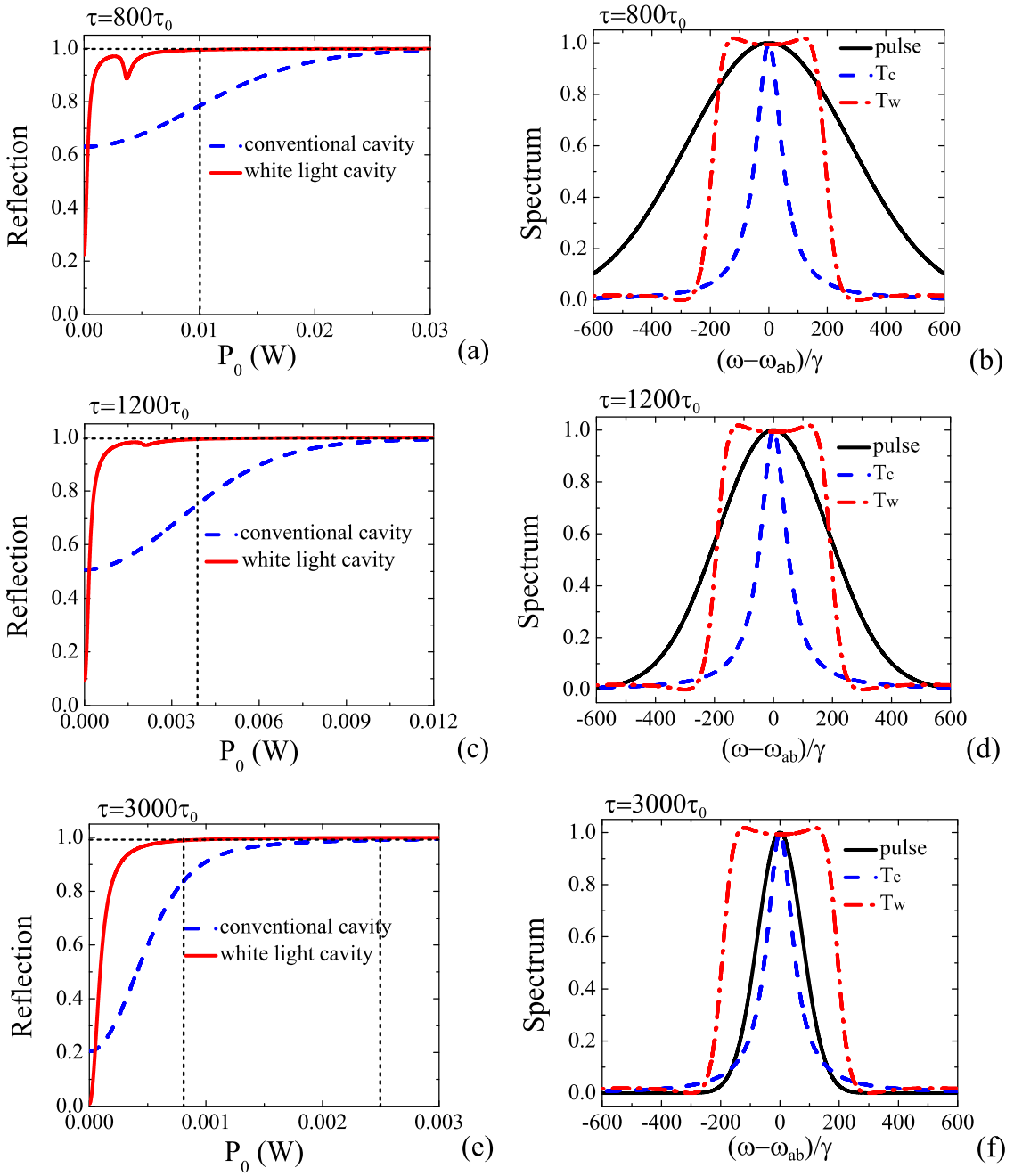

FIG. 5. Reflection of the pulse as a function of the input power when the duration of the pulse is (a) $\tau = 800\tau_0$, (b) $\tau = 1200\tau_0$, and (c) $\tau = 3000\tau_0$. Comparison among the spectrum of the pulse (black solid curve) and the transmission spectra of the conventional resonator T_c (blue dashed curve) and white-light cavity T_w (red dash-dotted curve) when the duration of the pulse is (b) $\tau = 800\tau_0$, (d) $\tau = 1200\tau_0$, and (f) $\tau = 3000\tau_0$.

and the transmission coefficient $t(\omega)$ is defined as

$$t(\omega) = \frac{E_t}{E_{\text{in}}} = \frac{t_1 t_2 e^{i\varphi_0/2}}{1 - r_1 r_2 e^{i\varphi_0}}. \tag{25}$$

The intracavity field intensity at C_2 is

$$I_{\text{intra}}(t) = \left(\frac{\tau}{2\sqrt{\pi}}\right)^2 \left| \int_0^\infty \sqrt{M_0(\omega)} e^{-\tau^2(\omega-\omega_0)^2/4 - i\omega t} d\omega \right|^2 = \frac{1}{|t_2|^2} I_t(t). \tag{26}$$

with intracavity amplification

$$\sqrt{M_0(\omega)} = \frac{t_1 e^{i\varphi_0/2}}{1 - r_1 r_2 e^{i\varphi_0}}. \tag{27}$$

Here the intracavity intensity relates to nonlinear effects according to Eq. (6). However, the intracavity pulse at C_2 follows the same evolution as the transmitted pulse; their ratio is $1/|t_2|^2$, which is just the Q factor. Therefore we can judge the switching time through the time delay needed to reach the maximum intensity of the transmitted pulse relative to that of the incident pulse.

We calculate the pulse evolution of the incident field at port A, the reflected field at port B, and the transmitted field at port C first in a conventional resonator. The results are shown in Fig. 6 for different pulses with durations $\tau = 800\tau_0$, $\tau = 1200\tau_0$, and $\tau = 10\,000\tau_0$.

For the input pulse with duration $\tau = 800\tau_0$, the transmitted pulse is weak and broad as shown in Fig. 6(a). This happens because the spectrum of the pulse is broader than the transmission spectrum of the ring cavity, shown in Fig. 5(b), and few parts of the pulse can enter into the cavity and finally transmit through it. The time decay for the peak value of the transmitted pulse is about $\tau_c = 850\tau_0$ which is much smaller than the predicted cw switching time.

For the case of an input pulse with $\tau = 1200\tau_0$, the ratio of frequency components resonant with the ring cavity increases as shown in Fig. 5(d). Therefore the transmitted pulse in Fig. 6(b) becomes stronger than that in Fig. 6(a). Meanwhile, the time decay for the peak value is prolonged to near $\tau_c = 1100\tau_0$ as shown in Fig. 6(b).

When the duration of the pulse increases to $\tau = 10\,000\tau_0$, the spectrum of the pulse is so narrow that it is resonant with the resonator as shown in Fig. 5(f). Therefore the transmitted pulse has nearly the same shape as the incident pulse, and the time decay for the peak value is about $2700\tau_0$ which is very close to the predicted time of the cw case $\tau_c = 3000\tau_0$. If we further increase the duration of the pulse, the switching time should approach $3000\tau_0$. Therefore Eq. (6) is valid for the cw case and is the limitation for a long pulse in the conventional ring resonator.

However, the white-light cavity not only reduces the switching power which is mentioned in the previous section, but also shortens the switching time compared to the conventional resonator. The reason is that the group velocity of the pulse in a white-light cavity is faster than that in a conventional resonator. It is known that the group velocity in a dispersive material is

$$\upsilon_g = \frac{d\omega}{dk} = \frac{c}{n(\omega) + \omega\frac{\partial n(\omega)}{\partial \omega}}. \tag{28}$$

For a white-light cavity, $\partial n/\partial\omega$ is negative as shown in Fig. 3. The denominator in Eq. (28) is therefore smaller than that in constant-index or positive-dispersive materials, i.e., conventional resonators, and this leads to a faster group velocity. Therefore the time needed to reach the peak value of the transmitted pulse in a white-light cavity is shorter than in a conventional cavity. This leads to a shorter switching time.

In Fig. 7, we plot pulse evolutions in a white-light ring cavity for input pulses with $\tau = 800\tau_0$, $\tau = 1200\tau_0$, and $\tau = 10\,000\tau_0$. The black solid curves refer to the input pulse, and the blue dashed curves refer to the pulse transmitted through the white-light cavity. For comparison, we also show the pulse transmitted through a conventional resonator as red dot-dashed curves in the same figures.

It is clear that the pulses transmitted through a white-light cavity are stronger than those through a conventional cavity which confirms the conclusions of the previous section, namely, the white-light cavity is helpful in reducing the switching power. Furthermore, the time needed to reach the peak value is also shorter than that in a conventional cavity. When $\tau = 800\tau_0$, the time needed to reach peak value is $120\tau_0$ for the white-light cavity and $850\tau_0$ for the conventional cavity as shown in Fig. 7(a). Similarly, for the case of an input pulse

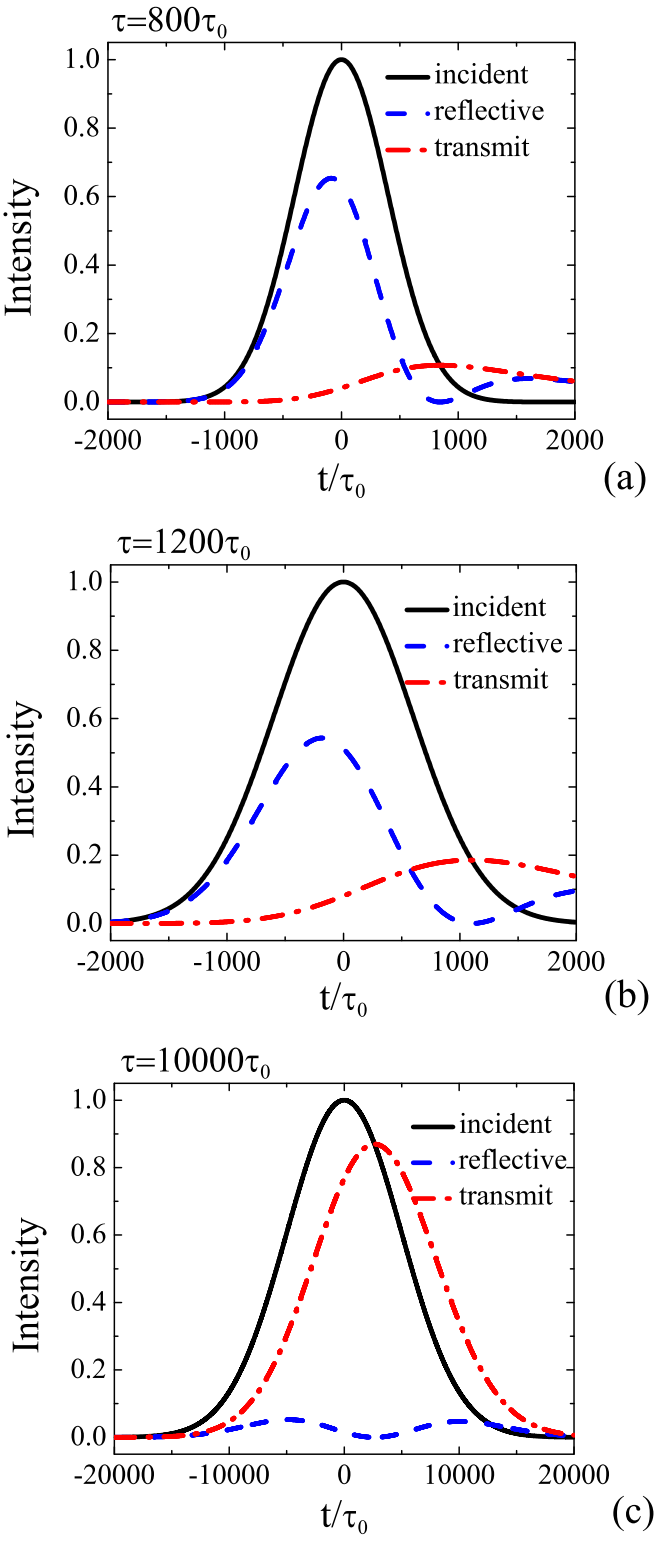

FIG. 6. Pulse evolution through a conventional ring cavity to check the switching time. The duration of the pulse is (a) $\tau = 800\tau_0$; (b) $\tau = 1200\tau_0$, and (c) $\tau = 10\,000\tau_0$, respectively. The black solid curves are incident pulses at port A; the red dash-dotted curves are the transmitted pulses at port C; the blue dashed curves are the reflective pulses at port B.

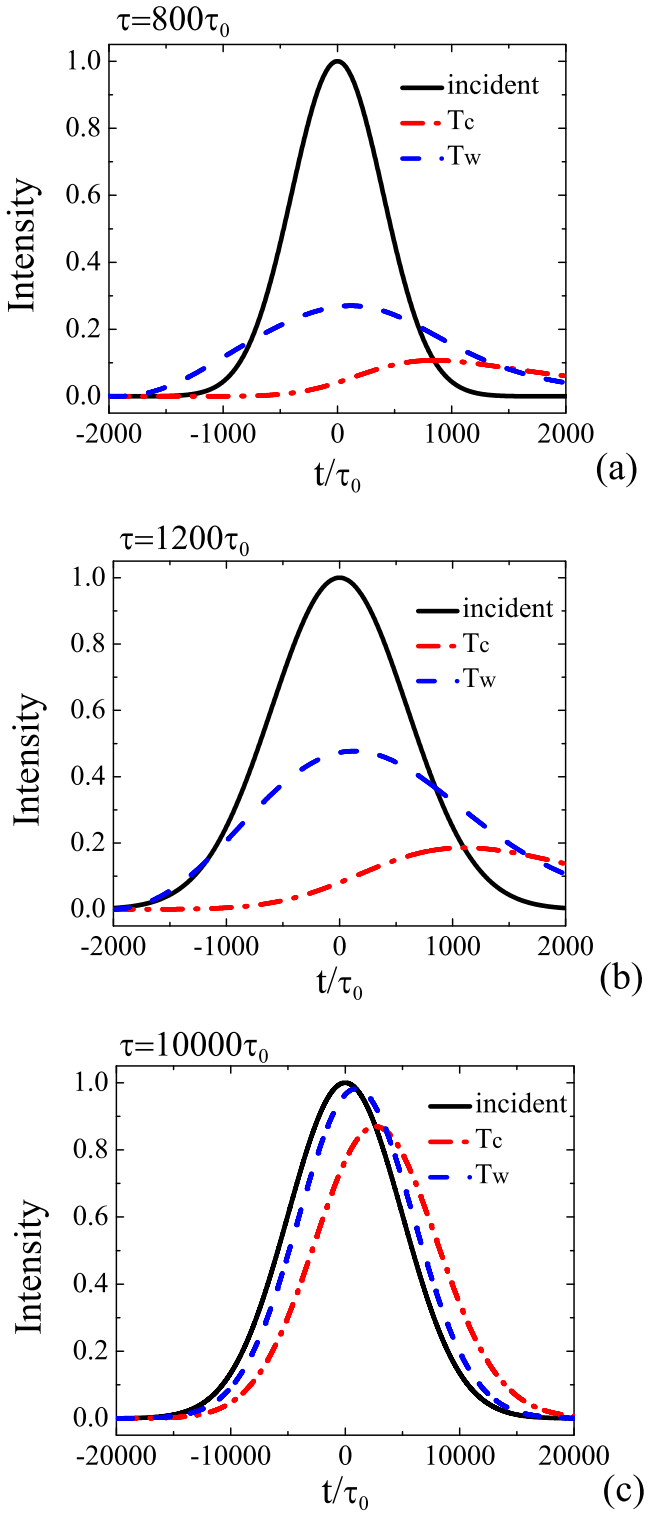

FIG. 7. Pulse evolution through a white-light ring cavity and a conventional ring cavity. The duration of the pulse is (a) $\tau = 800\tau_0$, (b) $\tau = 1200\tau_0$, and (c) $\tau = 10\,000\tau_0$. The black solid curves are incident pulses at port A; the red dash-dotted curves T_c are the transmitted pulses at port C for a conventional ring cavity; the blue dashed curves T_w are the transmitted pulses at port C for a white-light ring cavity.

with $\tau = 1200\tau_0$, the time needed to reach the peak value of the transmitted pulse is $130\tau_0$ for the white-light cavity and $1100\tau_0$ for the conventional cavity as shown in Fig. 7(b). When $\tau = 10\,000\tau_0$, the time needed to reach the peak value of the pulse transmitted through a white-light cavity is $1000\tau_0$, which is much shorter than $2700\tau_0$ in the case of a conventional cavity.

Combining Eqs. (28) and (15) we obtain an infinite group velocity at ω_0 in the white-light cavity in principle. However, the index of the fiber in a white-light cavity is complex, as shown in Fig. 3, even if the imaginary part at ω_0 is extremely small, and this prevents the infinite group velocity from being reached. Therefore, the time needed to reach the peak value of the pulse transmitted through the white-light cavity is not zero in the above calculations. In the case of Fig. 7(c), if we consider that the pulse runs 100 circles ($Q = 100$) before it escapes out at port C, the time delay $1000\tau_0$ indeed means superluminal, because $2000\tau_0$ is needed for a particle to run 100 circles with light velocity c in the fiber of $l = 20\lambda_0$. However, our result does not violate causality or special relativity. The negative-dispersion region between two gain peaks given in Eq. (13) is a result of the Kramers-Kronig relation which itself is based on the causality requirements of electromagnetic responses [28,29]. Meanwhile the superluminal group velocity of a pulse is just the result of reshaping, which results from the interference between different frequency components in an anomalous dispersion region as discussed in [28] [our Fig. 3 is very similar to the Fig. 1(b) in [28]]. The local velocity of energy propagation never exceeds c.

In summary, the nonlinear optical switch based on a white-light cavity can reduce the switching power and the switching time simultaneously unlike the case of a conventional ring resonator.

V. CONCLUSION

The all-optical switch is a pivotal technology in the field of photonics. The development of photonic information technology is in urgent need of a low-power-consumption, high speed, low-absorption, low-cost, and practical all-optical switch. All-optical switches have not been practical until now, because of a series of difficulties, the most important of which is that there is a fundamental issue relating to the switching power and the switching time. Generally speaking, the lower is the switching power, the longer is the switching time, and vice versa.

In this paper, we proposed a ring cavity doped with a group of three-level atoms such that the effective susceptibility can be adjusted to realize negative dispersion through incoherent pump and coherent driving fields. Through optimizing parameters to transform the conventional ring cavity into a white-light ring cavity, we can achieve a high-Q cavity with broadband resonance. When the incident field is a light pulse, the nonlinear optical switch based on the white-light ring cavity can reduce the switching power and improve the switching time simultaneously. The performance of the switch can be further improved if the broadband nature of the white-light cavity is improved. When the FWHM of the white-light cavity is doubled to that of a conventional resonator, the switching power and switching time can be reduced by more than half. If the FWHM of the white-light cavity is much larger than that of a conventional resonator, the switching power and switching time can be reduced to a level which is superior to the present electric switches. Therefore a switch based on a white-light cavity helps in overcoming the bottleneck associated with the

reciprocal relationship between the switching power and the switching time.

ACKNOWLEDGMENTS

This research was supported by the Joint Fund of the National Natural Science Foundation of China (Grant No. U1330203), the National Natural Science Foundation of China (Grants No. 11274242, No. 11474221, No. 11574229, and No. 11504272), the 973 program (Grant No. 2013CB632701), Shanghai Science and Technology Committee (Grant No. 15XD1503700), and the Shanghai Education Commission Foundation. The research of M.S.Z. is supported by NPRP (Grant No. 7-210-1-032) from the Qatar National Research Fund (QNRF).

[1] I. Glesk, R. J. Runser, and P. R. Prucnal, New generation of devices for all-optical communications, Acta Phys. Slovaca **51**, 151 (2001).

[2] C. Grezes, B. Julsgaard, Y. Kubo, W. L. Ma, M. Stern, A. Bienfait, K. Nakamura, J. Isoya, S. Onoda, T. Ohshima, V. Jacques, D. Vion, D. Esteve, R. B. Liu, K. Molmer, and P. Bertet, Storage and retrieval of microwave fields at the single-photon level in a spin ensemble, Phys. Rev. A **92**, 020301(R) (2015).

[3] D.-S. Ding, W. Zhang, Z. Y. Zhou, S. Shi, G. Y. Xiang, X. S. Wang, Y. K. Jiang, B. S. Shi, and G. C. Guo, Quantum Storage of Orbital Angular Momentum Entanglement in an Atomic Ensemble, Phys. Rev. Lett. **114**, 050502 (2015).

[4] N. Nozhat and N. Granpayeh, All-optical logic gates based on nonlinear plasmonic ring resonators, Appl. Opt. **54**, 7944 (2015).

[5] P. Urquhart, Compound optical-fiber-based resonators, J. Opt. Soc. Am. A **5**, 803 (1988).

[6] K. Ogusu, H. Shigekuni, and Y. Yokota, Dynamic transmission properties of a nonlinear fiber ring resonator, Opt. Lett. **20**, 2288 (1995).

[7] W. Yoshiki and T. Tanabe, All-optical switching using Kerr effect in a silica toroid microcavity, Opt. Express **22**, 24332 (2014).

[8] J. P. Cetina, A. Kumpera, M. Karlsson, and P. A. Andrekson, Phase-sensitive fiber-based parametric all-optical switch, Opt. Express **23**, 33426 (2015).

[9] A. Bananej and C. Li, Controllable all-optical switch using an EDF-ring coupled M-Z interferometer, IEEE Photon. Technol. Lett. **16**, 2102 (2004).

[10] J. E. Heebner and R. W. Boyd, Enhanced all-optical switching by use of a nonlinear fiber ring resonator, Opt. Lett. **24**, 847 (1999).

[11] C. Li, N. Dou, and P. Yupapin, Milliwatt and nanosecond all-optical switching in a double-coupler ring resonator containing an EDFA, J. Opt. A: Pure Appl. Opt. **8**, 728 (2006).

[12] T. Biwa, Y. Ueda, H. Nomura, U. Mizutani, and T. Yazaki, Measurement of the Q value of an acoustic resonator, Phys. Rev. E **72**, 026601 (2005).

[13] S. Sederberg, D. Driedger, M. Nielsen, and A. Y. Elezzabi, Ultrafast all-optical switching in a silicon-based plasmonic nanoring resonator, Opt. Express **19**, 23494 (2011).

[14] R. H. Rinkleff and A. Wicht, The Concept of white light cavities using atomic phase coherence, Phys. Scr. T **118**, 85 (2005).

[15] A.Wicht, K. Danzmann, M. Fleischhauer, M. Scully, G. Müller, and R. H. Rinkleff, White-light cavities, atomic phase coherence, and gravitational wave detectors, Opt. Commun. **134**, 431 (1997).

[16] S.Wise, G. Mueller, D. Reitze, D. B. Tanner, and B. F. Whiting, Linewidth-broadened Fabry-Perot cavities within future gravitational wave detectors, Class. Quantum Grav. **21**, S1031 (2004).

[17] M. S. Shahriar, G. S. Pati, R. Tripathi, V. Gopal, M. Messall, and K. Salit, Ultrahigh enhancement in absolute and relative rotation sensing using fast and slow light, Phys. Rev. A **75**, 053807 (2007).

[18] A. A. Savchenkov, A. B. Matsko, and L. Maleki, White-light whispering gallery mode resonators, Opt. Lett. **31**, 92 (2006).

[19] G. S. Pati, M. Salit, K. Salit, and M. S. Shahriar, Demonstration of a Tunable-Bandwidth White-Light Interferometer Using Anomalous Dispersion in Atomic Vapor, Phys. Rev. Lett. **99**, 133601 (2007).

[20] Q. Sun, M. S. Shahriar, and M. S. Zubairy, Effects of noise and parameter deviations in a bichromatic Raman white light cavity, Phys. Rev. A **81**, 033826 (2010).

[21] J. Zhang, X. Wei, G. Hernandez, and Y. Zhu, White-light cavity based on coherent Raman scattering via normal modes of a coupled cavity-and-atom system, Phys. Rev. A **81**, 033804 (2010).

[22] J. Xu, M. Al-Amri, Y. Yang, S.-Y. Zhu, and M. S. Zubairy, Wide-band optical switch via white light cavity, Phys. Rev. A **86**, 033828 (2012).

[23] H. Lu, Y. Jiang, and Z. Bi, Measurement of reflectivity of optical mirrors using laser phase modulation and fineness of fabry-perot cavity, Chin. J. Lasers **33**, 1675 (2006).

[24] R. A. Betts, T. Tjugiarto, Y. L. Xue, and P. L. Chu, Nonlinear refractive index in erbium doped optical fiber: theory and erperiment, IEEE J. Quantum Electron. **27**, 908 (1991).

[25] S. Asiri, J. Xu, M. Al-Amri, and M. S. Zubairy, Controlling the Goos-Hanchen and Imbert-Fedorov shifts via pump and driving fields, Phys. Rev. A **93**, 013821 (2016).

[26] J.-X. Zhang, H.-T. Zhou, D.-W. Wang, and S.-Y. Zhu, Enhanced reflection via phase compensation from anomalous dispersion in atomic vapor, Phys. Rev. A **83**, 053841 (2011).

[27] N.-H. Liu, S.-Y. Zhu, H. Chen, and X. Wu, Superluminal pulse propagation through one-dimensional photonic crystals with a dispersive defect, Phys. Rev. E **65**, 046607 (2002).

[28] L. J. Wang, A. Kuzmich, and A. Dogariu, Gain-assisted superluminal light propagation, Nature (London) **406**, 277 (2000).

[29] L. D. Laudau and E. M.Lifshitz, *Electrodynamics of Continuous Media* (Pergamon, Oxford, 1960).